Salt-Induced Polyelectrolyte Interdiffusion in Multilayered Films: A Neutron Reflectivity Study

Houssam W. Jomaa and Joseph B. Schlenoff*

Department of Chemistry & Biochemistry, and Center for Materials Research and Technology (MARTECH), The Florida State University, Tallahassee, Florida 32306

Received January 12, 2005; Revised Manuscript Received June 13, 2005

ABSTRACT: Polyelectrolyte multilayers were constructed from poly(styrenesulfonate), PSS, and poly(diallyldimethylammonium) with regularly interspersed layers of deuterated PSS. Annealing, by salt, of the fuzzy internal layering within this multilayer was followed using neutron reflectometry. A "limited source" diffusion model fit the data well and showed that polyelectrolyte migrates much more slowly within the bulk of a multilayer than at the surface. Enhanced surface mobility and a nonlinear increase in diffusion rate with salt concentration were explained by a salt doping model, where correlated short lengths of polyelectrolyte move by exchange with counterions ("extrinsic charge") doped into the ultrathin film of polyelectrolyte complex on exposure to solutions of high ionic strength.

Introduction

Since the boundaries between nominal "layers" in polyelectrolyte multilayers, PEMUs, are somewhat diffuse, due to interpenetration between positive and negative components, these thin films of complexed polyelectrolytes tend to be amorphous.[1,2] However, because polyelectrolyte mobility has a range limited to a few nanometers, it is possible to assemble chemically or isotopically distinct layers separated by several layers of different composition.[3] Labeling of sulfonated polyelectrolyte by deuterium, for example, has permitted a detailed perspective on the "fuzzy" nature of PEMU structuring.[4−6]

The linear, layer-by-layer, growth mode of PEMUs, though widely appreciated and exploited, is an inherently nonequilibrium process, yielding nonequilibrium structure.[7−9] In the adsorption process itself, individual molecules attach to the surface of a growing PEMU via many ion pairing contacts.[10] Unless the polyelectrolyte molecules are small, or weakly interacting (as might be the case in the presence of high salt concentration), the adsorption is kinetically irreversible on the time scale of the PEMU assembly.[10,11] Because the thickness increment ("layer" thickness) quickly becomes independent of total thickness, it is reasonably assumed that the adsorbing polyelectrolyte becomes locked in place, notwithstanding some short-range interdiffusion. Recent work has challenged the notion of frozen or immobile polyelectrolytes within multilayers. For example, nonlinear or "exponential" growth of multilayers[12−19] is evidence that one or more polyelectrolytes is able to diffuse throughout the film, rather than being held static on a local level. Exchange of multilayer for solution polyelectrolyte is further proof of mobility within multilayers capable of exponential growth.[16] Large scale rearrangements within multilayers, from phase separation[20] to decomposition,[21−24] may be induced by changing the interactions between polymers with variations of ionic strength or pH (if the polymer is a weak acid/base). In recent atomic force microscopy (AFM) work,[25] we showed that swelling of PEMUs by salt frees polyelectrolyte segments and allows polymer interdiffusion, leading to smoothing of the surface. The AFM work also recognized the strong nonlinear dependence of interdiffusion on degree of swelling, or "doping", by salt ions.[25] The introduction of salt counterions, or "extrinsic charge",[26,27] within PEMUs is represented by the following equilibrium:[28]

$$\mathrm{Pol^+Pol}_m^- + y\mathrm{Na}_{aq}^+ + y\mathrm{Cl}_{aq}^- \rightleftharpoons (1-y)\mathrm{Pol^+Pol}_m^- + y\mathrm{Pol^+Cl}_m^- + y\mathrm{Pol^-Na}_m^+ \quad (1)$$

where Pol^+ and Pol^- are respective positive and negative polyelectrolyte repeat units. y is the fraction of the multilayer in the extrinsic form, and $1 - y$ is the intrinsic fraction. The subscript "m" refers to components in the multilayer phase. While it is clear that salt moderates interpolyelectrolyte interactions, and therefore mobility,[25,29] as has been known for some time for both solution-precipitated polyelectrolyte complexes (PECs)[30−32] and polyelectrolyte adsorption to charged surfaces,[33,34] salt-controlled mobility of polyelectrolyte within the bulk of a PEMU remains largely unexplored. AFM measurements of PEMU topology only reveal salt-induced migration of polyelectrolyte on the surface[25,35] (which is, as will be shown below, quite distinct from bulk interdiffusion).

The principal tools for evaluating layering within PEMUs have been neutron or X-ray structural studies.[2−6,36−42] For example, Lösche et al. described a detailed neutron reflectometry study of poly(styrenesulfonate)/poly(allylamine), PSS/PAH, multilayers.[6] In this system, deuterated PSS layers were interspersed with nondeuterated layers in a regular fashion during the multilayering process.[6] Estimates were made of the range over which a nominal layer of polyelectrolyte was distributed. It was shown that neighboring layers interpenetrate, leading to an amorphous structure, unless deuterated layers were separated by a sufficient number of nondeuterated layers.[6] While deposition conditions were varied to obtain a range of fuzzy layer thicknesses, postdeposition mobility within PEMUs was not evaluated. In the present paper, we present neutron reflec-

* Corresponding author: Fax (850)644-3810, e-mail: schlen@chemmail.chem.fsu.edu.

10.1021/ma050072g CCC: $30.25
Published on Web 09/02/2005

Scheme 1. Structures of Polyelectrolytes Used for Multilayer Buildup[a]

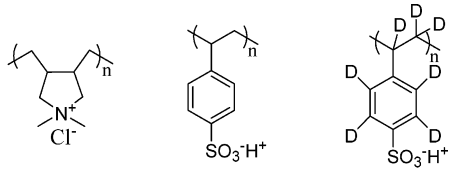

PDADMAC PSS d-PSS

[a] From left to right, poly(diallyldimethylammonium chloride), poly(styrenesulfonate), and deuterated poly(styrenesulfonate).

tometry modeling of PSS/poly(diallyldimethylammonium) PEMUs containing deuterated PSS layers. We then demonstrate that the addition of extrinsic charge, by swelling in salt solutions postassembly, further lubricates polyelectrolyte interdiffusion and erases the fuzzy layering present.

Experimental Section

Materials. Poly(diallyldimethylammonium chloride) (PDADMAC, Aldrich; $M_w = 3.69 \times 10^5$, $M_w/M_n = 2.09$), poly(styrenesulfonate) (PSS, Scientific Polymer Products; $M_w = 57\,500$, $M_w/M_n = 1.03$), and poly(ethylenimine) (PEI, Aldrich; $M_w \sim 7.5 \times 10^5$) were used as received. Deuterated polystyrene ($M_w = 63\,000$, $M_w/M_n = 1.2$) was purchased from Polymer Source and sulfonated to produce a deuterated polyelectrolyte. NaCl for annealing was from Fluka. All solutions were made with 18 Mohm deionized H_2O. Structures of polyelectrolytes used are shown in Scheme 1.

Sulfonation. Deuterated poly(styrenesulfonate) (d-PSS) was synthesized from deuterated polystyrene, d-PS. 0.1 g of d-PS was heated in 10 mL of 98% sulfuric acid at 90 °C for 15 h.[8] The product was diluted to 50 mL with distilled water and cooled to room temperature. The product was dialyzed against water using 3500 molecular weight cutoff dialysis tubing (SPEC) for 24 h. FTIR analysis of the product indicated a sulfonation level of at least 96%. Quasielastic light scattering gave a single-exponential decay for the correlation function and a hydrodynamic radius of 16.8 nm at zero salt concentration, showing that the polyelectrolyte was not cross-linked.

Polymer Characterization. Size exclusion chromatography−multiangle light scattering (SEC-MALS) measurements were performed at 25 °C using an Agilent 1100 series pump in series with a SEC column coupled to a DAWN-EOS light scattering detector (Wyatt Technologies) equipped with a He−Ne laser ($\lambda_0 = 690$ nm) and a Wyatt Optilab-DSP interferometric refractometer. SEC was performed with a 17 μm polymer column (300 mm × 7.5 mm, TSK Gel G5000PW, Tosoh Biosciences, covering the molar mass range 4000 g mol^{-1} to 1 × 10^6 g mol^{-1}) in series with a TSK-GEL guard column. The mobile phase was 50 mM phosphate buffer (pH = 7.14) with 50 mM NaCl and 200 ppm of NaN_3 (added as a preservative). Injections were 50 μL of 0.5 wt % polymer solution. The sample specific refractive index increment, dn/dc, was determined offline using Wyatt's DNDC version 5.2. Data were acquired and handled with Astra 4.81.07. The DAWN-EOS instrument was calibrated with toluene. A 50K dextran standard (Fluka) was used to normalize the fixed angle detectors on the DAWN-EOS and to verify performance of the SEC-MALS system (this standard was determined to be 5.06×10^4 g mol^{-1}, $M_w/M_n = 1.05$).

Multilayer Buildup. Polished silicon wafers, 3 in. diameter, were coated with ca. 30 Å of Cr followed by ca. 120 Å of gold, modified with a monolayer of octadecanethiol,[43] and then used as substrates for multilayer buildup. PEMU buildup started with one layer of PEI. Polyelectrolyte solutions for multilayer assembly were 1.0 mM (polyelectrolyte concentrations are based on the repeat unit) PDADMAC in 0.1 M NaCl, 1.0 mM PSS in 0.1 M NaCl, and 5.0 mM d-PSS in 0.1 M NaCl. Automated multilayer buildup was performed on a robotic platform (StratoSequence, nanoStrata Inc.) modified to accommodate the immersion of 3 in. diameter wafers, face down while spinning on the end of a vacuum chuck, into large beakers. Wafers were rotated at a speed of 700 rpm in an effort to make the multilayers as smooth and uniform as possible. Dipping in each polyelectrolyte solution was for 10 min, followed by three rinses in distilled water, 45 s each. The PEMU film was composed of 5 layers of d-PSS, each layer separated by 4.5 layer pairs of undeuterated material, and capped with a layer pair of undeuterated material. The system is represented by, starting with the silicon substrate on the left, Si/Cr/Au/$C_{18}H_{31}S$/PEI/PSS{(PDADMA/PSS)$_4$(PDADMA/d-PSS)}$_5$(PDADMA/PSS) @ 0.1 M NaCl. The multilayer was capped with nondeuterated polymer so that all d-PSS layers experienced the same environment. Thus, the total number of layers was 52 with 23.5 bilayers of PDADMA/PSS and 5 layers of d-PSS. The PEMU was dried with a gentle stream of nitrogen and maintained in ambient conditions for 1 week before structural studies started. The thickness of the multilayer directly after buildup was measured under ambient conditions (ca. 25% relative humidity and 25 °C) with a Gaertner Scientific L116S ellipsometer at an incident angle of 70° and was found to be 1350 Å. The rms surface roughness of the thin film was measured with an atomic force microscope (Digital Instruments, Dimension 3100 head and Nanoscope IV controller).

Neutron Reflectometry. The neutron reflectivity of the PEMU described above was measured using the Advanced Neutron Diffractometer and Reflectometer (AND/R) at the NIST Center for Neutron Research. The instrument is located at the NG-1 cold neutron beam guide and has a horizontal scattering geometry (vertical sample) in which the beam is defined by a pair of variable slits both upstream and downstream from the sample. The neutron wavelength, selected by a focusing pyrolytic graphite monochromator, is 5.0 Å with a bandwidth of ~1%. Higher harmonics are removed in an upstream Be filter operated at 77 K. The current instrument setup accepts sample sizes up to 3 in. in diameter. At low momentum transfer ($q_z < 0.022$ Å^{-1}), the slits were kept constant, which led to sample over-illumination at $q_z < 0.0075$ Å^{-1}. Above $q_z = 0.022$ Å^{-1}, the slit openings were kept proportional to the scattering angle Θ, resulting in a constant beam footprint on the sample and a constant instrument resolution of $\Delta q_z/q_z \sim 0.0136$. At this resolution, the neutron flux at the sample position is typically 3×10^4 counts cm^{-2} s^{-1}. The incident beam is monitored with a 1 in. pencil detector located after slit 1. The signal is determined in a 1 in. pencil detector located ~1.72 m (68 in.) after the sample. Isotropic background in the guide hall is shielded from the detector and amounts to less than 1 count/min. Incoherent background from the sample at larger q_z is measured by detuning the 2Θ arm of the instrument by $\Delta\Theta_{out} = +2.5°/-1.5°$. Background subtraction and footprint corrections were made using the *reflred* software provided by NIST. After data reduction, reflectivity for the dry multilayer was fitted with a composition profile using Parratt 32 (v. 1.5 HMI Berlin).

After collecting the first spectrum, the multilayer was reassembled in a housing that sandwiched the Si-supported PEMU between two silicon plates with a flow through jacket that allowed bathing the multilayer in aqueous media. The multilayer was then subjected to 0.8 M NaCl for different time intervals, specifically 10, 25, 55, 110, 170, and 260 min, rinsed with 18 Mohm water and then dried with an argon stream for 2 h. Reflectivity spectra were then collected under Ar after every salt bath, and data for multilayer annealing were obtained. The starting multilayer thickness obtained from neutron reflectivity is lower than the one reported by ellipsometry because the latter was obtained directly after assembly in a more humid atmosphere; thus, the film is more hydrated.

Discussion

Multilayer Character. Deuterated PSS was critical to establishing contrast for neutron scattering. Several methods are available, and were evaluated, for sulfonat-

ing polystyrene. For example, a "soft sulfonation" technique relies on the use of acetyl sulfate in 1,2-dichloroethane.[44] We were concerned that this approach would leave substantial portions of styrene repeat units unsulfonated. We therefore resorted to a harsher method, which we have used for isotopic labeling in the past.[8] The deuterated PSS ($M_w = 1.12 \times 10^5$, $M_w/M_n = 1.05$ after sulfonation) was about twice the M_w and of similar M_w/M_n compared to the unlabeled PSS. The PDADMA sample chosen had a broad molecular weight distribution and a small amount of branching, typical for commercial samples made from radical polymerization to high conversion of diallyldimethylamine. In our hands, branched and unbranched PDADMA give multilayers of similar thickness when prepared under the same conditions.[9]

A great deal of effort was expended in optimizing the deposition protocol. Sample uniformity across the 3 in. wafer, as well as low surface roughness, is essential. Roughness at the air/multilayer interface leads to poor quality reflectograms, in particular, to a reduced number of Kiessig fringes (which result from interference between neutrons reflected at the sample/PEMU and PEMU/air interfaces) and Bragg peaks (due to periodic layers of neutron contrast material in the PEMU). Several years ago we introduced the spinning of silicon wafers during PEMU deposition as a means to produce high-quality samples rapidly.[10] We modified our deposition robot to accommodate larger wafers using a vacuum chuck holder. A spinning rate of 700 rpm represented the maximum speed without undue turbulence. The 52-layer PEMUs were ~1207 Å thick when measured by ellipsometry in ambient (compare this value with 1190 Å estimated from reflectometry) and had thickness variations of ±6 Å (i.e., 0.5%) over the entire surface, up to 2 mm from the edge, as measured by an ellipsometer. More telling, they were completely uniform in color to the eye. The rms surface roughness, determined by AFM over a 1 μm × 1 μm area, was 2.1 nm.

Structural Model. The multilayer contains five equally spaced strata of d-PSS. Neutron reflectivity curves of the starting multilayer were collected on as-deposited samples before annealing in salt solutions. The uppermost spectrum in Figure 1 presents the low-q_z regime of an as-deposited multilayer under ambient conditions showing total external reflection of the Si substrate at $q_z < 0.01$ Å^{-1} and a set of well-developed Kiessig fringes.[45] A rough evaluation of the total PEMU thickness from the spacing of these fringes, $D_{film} = 2\pi/\Delta q_z$,[45] yields an estimate of $D_{film} \sim 1190$ Å. Moreover, a well-developed Bragg peak at $q_z \sim 0.028$ Å^{-1} indicates that d-PSS layers within the freshly prepared PEMU structure are well-defined and regularly spaced. The Bragg positions indicate a distance between the (centers of the) buried deuterated layers of d-PSS, $D_{int} \sim 220$ Å. We did not observe Bragg reflections beyond the second Bragg peak in this sample, indicating that the positional correlation between the deuterated layers was poorer than that in earlier work.[6] The internal roughness σ_{int} between the deposited layers cannot be established with high precision from the limited q_z range of the data. Modeling of the data (see below) suggested $\sigma_{int} = 12$ Å. Using a $\sigma_{int} = 15$ Å caused considerable deterioration to the fit. Earlier structural work on PSS/poly(allylamine hydrochloride) (PAH) multilayers[4] established $\sigma_{int} = 19 \pm 1$ Å for that system.

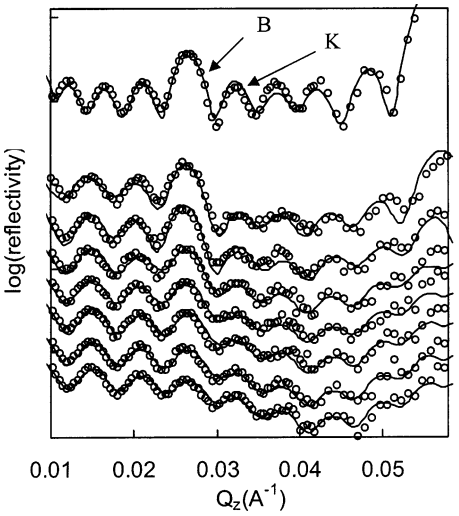

Figure 1. Plot of log(reflectivity) vs Q. Experimental data (open circles) and fit (solid line) of [(PDADMA/PSS)$_4$(PDADMA/d-PSS)]$_5$(PDADMA/PSS) multilayer. Uppermost curve: as-deposited sample measured in ambient. Lower curves, measured under argon (from top to bottom): after annealing (for 10, 25, 55, 110, 170, 260 min) in 0.8 M NaCl. A final anneal in 1 M NaCl for 120 min (lowest spectrum) almost completely removes the Bragg peak, B, to leave a Kiessig fringe, K.

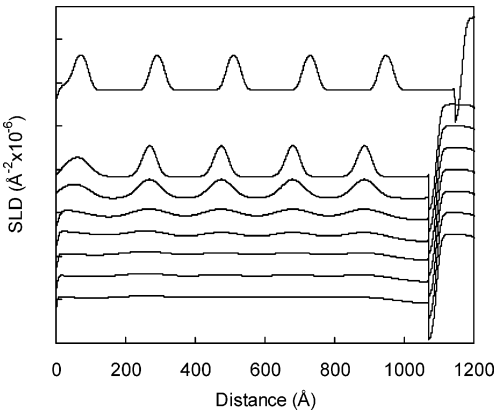

Figure 2. Plot of the scattering length density vs distance from the air/PEMU interface. Samples as in Figure 1. Increases in SLD are due to deuterated layers. The deuterated stratum closest to the surface dissipates faster than the rest, consistent with the finding of enhanced surface diffusion.

SLD profiles were fit for all curves and are presented, with a slope correction and offset, in Figure 1. Corresponding profiles for deuterated material are presented in Figure 2.

In constructing the profiles, we are able to incorporate several pieces of published information[4−6] regarding polyelectrolyte multilayers. As seen in earlier work,[4,6] the rather slight neutron scattering contrast between nondeuterated layers in a PEMU system does not leave a signature in the reflection spectra. Also, in earlier structural characterization of PEMUs with X-ray and neutron scattering,[4,6] it was assumed that the interface between sequential layers is blurred with a line shape that follows an error function. This assumption led to a satisfactory description of the data. Since a detailed experimental determination of this line shape is beyond the limits of resolution, the chosen functional description is as good as any and has the advantage of converging toward an overall Gaussian line shape if the roughness parameter σ_{int} is of the order of the layer thickness (which is the case for the d-PSS layers).

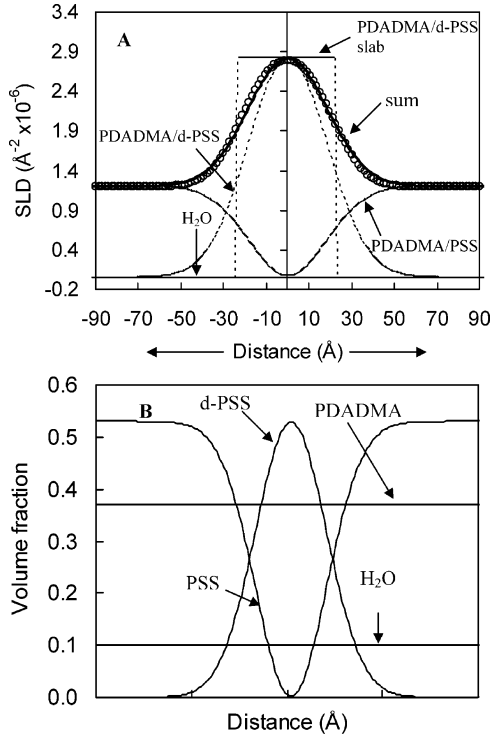

Figure 3. (A) SLD contributions of individual components making up the multilayer through one PDADMA/d-PSS stratum (components as labeled on the graph). The solid line, representing the sum of all components, is a Gaussian with $\sigma_0 = 18.5$ Å. The open circles represent the profile of the multilayer generated by the fitting routine (taken from Figure 2). (B) Concentration profile, in terms of volume fraction vs distance, of components through one PDADMA/d-PSS stratum as in (A). Corresponding contributions are marked in the figure.

Table 1. Composite SLD Values for Blended Polyelectrolytes in the Multilayer

material	effective SLD ($Å^{-2} \times 10^{-6}$)
PDADMA/d-PSS	2.77
PDADMA/PSS	1.15

Additional information for the model included the finding that the polyelectrolyte complex within the PEMU is essentially counterion-free.[11,46,47] This "intrinsic compensation" of polymer charge guarantees a 1:1 blending, at the molecular level, of polyelectrolyte repeat units. Direct FTIR measurements on thick (several micrometers) PSS/PDADMA multilayers[47] placed an upper limit of about 6 mol % on counterion content. Approximately the same value was obtained for thick PSS/PAH films.[48] Thin PEMU films contain even fewer counterions.[11] The composition of PDADMA is therefore assumed to be uniform, and at all points within the film, poly(styrenesulfonate), whether deuterated or not, is diluted 1:1 (on a repeat unit basis) by PDADMA. Such a distribution allows one to represent material between d-PSS layers as a homogeneous blend of PSS and PDADMA. The term "stratum" is used to denote blended layers of d-PSS and PDADMA or PSS and PDADMA.

Scattering length densities (SLDs) of pure components are provided in the Supporting Information. SLDs of blended polyelectrolytes existing in strata are provided in Table 1.

Shown in Figure 3 is a cross section through one of the strata of PDADMA/d-PSS in the as-prepared film, where individual contributions to the total SLD are presented, as well as their sum. Note that since this first sample was recorded in ambient, 10 vol % water is included. Although the SLD contribution of water itself is small, it makes a significant contribution to the SLD profile by virtue of the fact that it dilutes other components. For all samples, PDADMA is assumed to be uniformly distributed, as stated above. The contributions of PSS and d-PSS, at distance z from the substrate, follow the mass balance law (molar concentrations used)

$$[\text{PDADMA}]_z = [\text{PSS}]_z + [\text{d-PSS}]_z = \text{constant} \quad (2)$$

While the purpose of the present work is not a detailed structural characterization, as suggested by the fits of the reflectivity models overlayed on the experimental data in Figures 1 and 2, these fits and approximations are quite reasonable. The independent model parameters that were adjusted in these fits were the thickness and SLD of a PDADMA/d-PSS stratum, $d_{\text{PDADMA/d-PSS}}$ and $\rho_{\text{PDADMA/d-PSS}}$, and the thickness and SLD of a PDADMA/PSS stratum, $d_{\text{PDADMA/PSS}}$ and $\rho_{\text{PDADMA/PSS}}$ (all above-mentioned layers are repeated 5 times). The thickness and SLD of the base layers (Cr, Au, and alkanethiol), d_{Cr}, ρ_{Cr}, d_{Au}, ρ_{Au}, d_{C18}, ρ_{C18}, were provided by the experimental conditions and calculated using the NIST online SLD calculator (http://www.ncnr.nist.gov). The parameters of the outer PDADMA/PSS bilayer, d_{out} and ρ_{out}, exert only marginal influence on the model and were only varied slightly in the model to obtain the best fit.

Fits for upper curves shown in Figures 1 and 2 employed the following: $d_{\text{PDADMA/PSS}} = 178$ Å, $d_{\text{PDADMA/d-PSS}} = 44.3$ Å, $d_{\text{out}} = 45.0$ Å, $d_{\text{Cr}} = 29.4$ Å, $d_{\text{Au}} = 124.0$ Å, and $d_{\text{C18}} = 21$ Å. Hence, we obtain $D_{\text{film}} \sim 1110$ Å, consistent with the semiquantitative estimates given above. The maximum SLDs of the PDADMA/PSS strata and PDADMA/d-PSS strata within the repeat sequence are $\rho_{\text{PDADMA/PSS}} \sim 1.15 \times 10^{-6}$ Å^{-2} and $\rho_{\text{PDADMA/d-PSS}} \sim 2.87 \times 10^{-6}$ Å^{-2}. While the exact SLD values are irrelevant for our purpose (and are coupled with the parameter σ_{int} whose value cannot be derived from the data collected over a relatively narrow q_z range), it is the contrast, $\Delta\rho_n = \rho_{\text{PDADMA/d-PSS}} - \rho_{\text{PDADMA/PSS}}$, that determines the height of the Bragg peak at a given (fixed) $d_{\text{PDADMA/d-PSS}}$ and σ_{int}. Additional model information is provided as Supporting Information.

The general features of the best-estimate profiles in Figure 2 have similarities and differences compared to reported multilayer profiles.[4,6] As deduced for d-PSS/PAH,[4,6] the deuterated strata are evenly spaced and the material in one layer spreads out beyond its nominal location. However, no stratification of PDADMA is invoked in our model, as it is uniformly blended with polyanion. Furthermore, the distribution for PDADMA/d-PSS is the narrowest Gaussian that can be drawn using the material in the rectangular slab of PDADMA/d-PSS blend that represents an idealized "layer" of deuterated material (shown in Figure 2).[49] At the center of the peak there is no PSS.

Annealing by Salt. Following buildup, the multilayer was immersed in salt solutions to promote ion doping and interdiffusion ("annealing") of polyelectrolytes within the bulk PEMU. From prior AFM studies of surface annealing in PDADMA/PSS it is known that at least 0.5 M NaCl is required to effect appreciable structural rearrangements.[25] In the present studies, 0.5 M NaCl proved insufficient to induce bulk polymer movement on a time scale of hours, and thus the salt

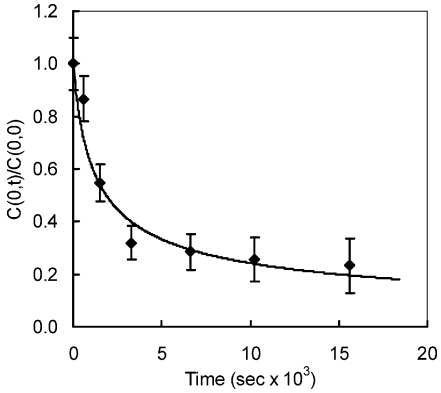

Figure 4. Plot of relative d-PSS concentration at the profile peak maximum vs time and the corresponding fit using eq 5 and appropriate values for σ_0 and D (solid line).

concentration was increased to 0.8 M. Reflectograms were recorded (Figure 1, lower curves) in a dry argon atmosphere after successive annealing and rinsing steps. At the end of the annealing period, the multilayer was immersed in 1.0 M NaCl for 120 min. This final treatment almost completely removed all trace of the Bragg peak. It is assumed that no polyelectrolyte diffusion occurs during the times the wafer is either immersed in pure rinse water or is scanned ex-situ.

The intensity of the Bragg peak in Figure 1 decreases with time of exposure to 0.8 M NaCl, evidence of steadily diffusing structure. The reflectivity scans for the annealed samples, recorded under argon, are shifted along the Q axis compared to the starting as-made sample because the latter was recorded under ambient conditions and contained about 10 vol % water. This water content is entirely consistent with prior FTIR studies of hydration within these PEMUs and causes the film to be about 10% thicker than the dry ones.[50] Fit parameters for annealed samples are provided in the Supporting Information.

Kinetic information on polyelectrolyte chain movement within the thin film was obtained by following the intensity of the Bragg peak vs time or the SLD profile vs time in Figure 2. After extensive annealing, the Bragg peak appears to have substantially disappeared, with a residual intensity of a few percent suggested by the fitted profiles. Neutron reflectograms were converted to SLD profiles (Figure 2) from which the concentration of d-PSS was extracted. Concentrations of d-PSS at the peak, relative to the initial concentrations, are plotted vs time in Figure 4. The first point at $t > 0$ deviates from the fit, possibly because of a short "induction period", observed in prior studies on surface diffusion in PEMUs[25] or possibly because the initial material distribution is "fatter" than Gaussian and requires a little time to assume a more Gaussian shape.

The movement of polyelectrolyte under annealing was modeled as "limited source diffusion", which assumes a band of material having a Gaussian distribution diffuses in a direction perpendicular to the band, as follows:[51]

$$C(x,t) = \frac{Q_0}{(4\pi Dt + 2\pi\sigma_0^2)^{1/2}} \, e^{-x^2/(4Dt+2\sigma_0^2)} \qquad (3)$$

where $C(x,t)$ is the concentration of the deuterated polymer (mol/cm^3) in one stratum at distance x from the center of the band at time t, Q_0 is the amount of d-PSS deposited per unit area in one layer, and σ_0 is the standard deviation of the initial layer. D is the interdiffusion coefficient of d-PSS. Since d-PSS only differs (to a first approximation) from PSS by being isotopically labeled, and PDADMA is uniform throughout, D should remain constant. At $t = 0$ we have the initial conditions

$$C(x,0) = \frac{Q_0}{(2\pi\sigma_0^2)^{1/2}} \, e^{-x^2/2\sigma_0^2} \qquad (4)$$

Hence, the relative concentration at the center of the band (the maximum of the Gaussian) is given by

$$\frac{C(0,t)}{C(0,0)} = \frac{(2\pi)^{1/2}\sigma_0}{(4\pi Dt + 2\pi\sigma_0^2)^{1/2}} \qquad (5)$$

σ_0 is taken from the initial model (Figure 2, $\sigma_0 = 18.5$ Å), and D is the only unknown. In Figure 4, a plot of eq 5, using a diffusion coefficient of 2.9×10^{-17} cm^2 s^{-1}, provides an acceptable fit. In view of the uncertainties in σ_{int} and other experimental errors, realistic values for D fall between 2×10^{-17} and 6×10^{-17} cm^2 s^{-1}.

A diffusion coefficient of ca. 10^{-17} cm^2 s^{-1} is 3−4 orders of magnitude smaller than diffusion coefficients estimated from AFM studies of salt-induced annealing using the same polyelectrolyte system.[25] For example, in the AFM work,[25] 1.0 M NaCl yielded polyelectrolyte interdiffusion coefficients of ca. 5×10^{-14} cm^2 s^{-1}. (Studies on the diffusion of proteins on multilayers yield diffusion coefficients of order 10^{-10} cm^2 s^{-1}.[52]) The difference is that AFM visualizes surface topology, and changes thereof, which stem from surface diffusion, whereas the neutron study of the present work reveals bulk mobility. (Extrapolating from our earlier AFM results, we initially tried to anneal deuterated multilayers with 0.5 M salt and were surprised to find no changes in structure over the course of several hours.) Differences in surface and bulk diffusion coefficients for small molecules were reported by Klitzing and Möhwald.[27] For example, the surface diffusion of Rhodamine in PAH/PSS was 1−2 orders of magnitude greater than in the bulk.

A rationalization of the difference between bulk and surface diffusion, as well as the general question of polyelectrolyte interdiffusion and the role of salt counterions, may be reached by considering the microscopic picture for the mechanism. As-deposited (with a final rinse in distilled water) polyelectrolyte multilayers contain few salt counterions—internal charge is balanced by matched numbers of positive and negative polymer repeat units ("intrinsic" compensation). We have measured the residual ion content ("extrinsic" charge) in much thicker PDADMA/PSS films to be about 6 mol % before annealing and about 2 mol % after annealing.[47] In the limit, with no extrinsic charge compensation, a polymer chain with n charged repeat units forms n ion pairs and therefore adheres very tightly to its oppositely charged partner(s). To a first-order approximation, the interaction energy, ΔF, between two polymer chains scales as ξn, where ξ is the association energy for one ion pair.[53−55] In reality, this scaling only holds for n up to about 10, whereupon the binding cooperativity represented by this scaling dissipates.[54,55]

At the intrinsic limit, movement of part or all a polyelectrolyte molecule is difficult. For two rodlike oppositely charged polyelectrolytes, all ion pairs would

Scheme 2. Movement of Polyelectrolyte Segments within a Polyelectrolyte Complex[a]

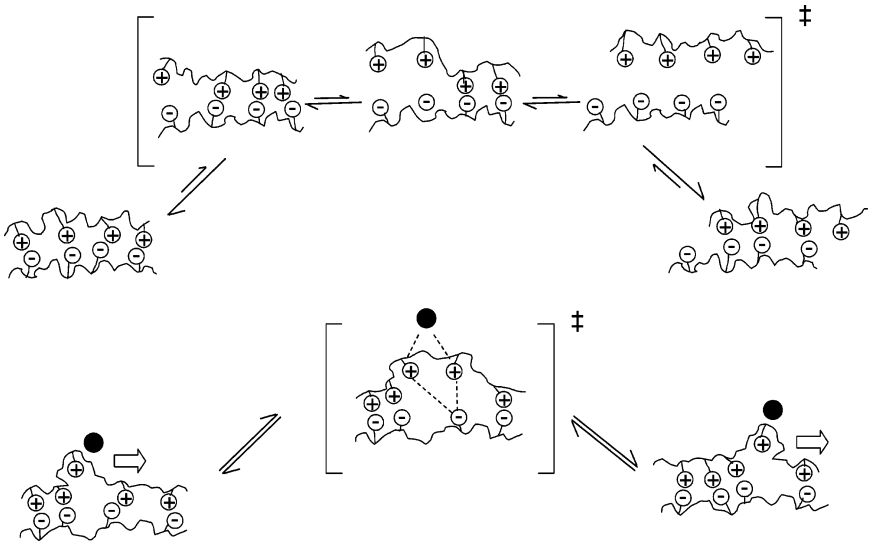

[a] In the upper path, several ion-pairing contacts must break before the segment moves. In the lower path, participation of an extrinsic charge (solid dot, a negative counterion in this example) allows localized place-exchange of individual repeat units, or a small group of them. Suggested transition states are depicted.

have to be disengaged simultaneously in order to move a polymer chain. For flexible polymers, such as the present case, short runs of adjacent repeat units are able to act in a localized fashion, and if a sufficient number of ion pairs are simultaneously unpaired, a correlated group of units might be able to move in concert, as illustrated by Scheme 2. In Scheme 2, a group of adjacent intrinsic ion pairs has sequentially dissociated, moved, and reassociated. As the probability for each dissociation step is low, the probability of achieving the simultaneous dissociated condition shown in the transition state in the Scheme is much lower.

Shown in the lower half of Scheme 2 is a representation of interdiffusion if extrinsic charge enters the picture: one of the positive polyelectrolyte charges is extrinsically compensated by a salt anion (such as chloride). The chloride ion facilitates the local rearrangement of the polyelectrolyte by hopping with the polyelectrolyte segment as it moves. The transition state drawn in the lower pathway in Scheme 2 merely suggests a way that the energy barrier for hopping can be minimized by concerted participation of four charged species (connected by dotted lines).

Because of bond restrictions and connectivity, motions of polyelectrolyte segments are coupled, and it is likely that several adjacent repeat units on a chain, with the participation of several counterions, undergo a quasi-concerted localized reshuffling to end up with net polymer motion. The group of adjacent units that actually moves (via self-diffusion under a concentration gradient) is characterized by an equivalent or effective cooperative binding length, λ_{eq}, that depends, among other factors, on the flexibility of the polyelectrolyte backbone. To make a rough estimate of this length, we refer to important work by Tsuchida and Osada,[55] who evaluated the binding of poly(methacrylic acid) to poly(quaternary ammoniums) as a function of chain length of the latter species. Binding cooperativity, and its rapid decay, was demonstrated. From the results of Tsuchida,[55] extrapolating from the linear $\Delta F \sim \xi n$ regime (at low n), after a poly(quaternary ammonium) chain has reached a length of about 8 units, the binding energy per segment plateaus. Since there are two ends to each chain, we estimate λ_{eq} to be about 4 units—seemingly short—but it should be remembered that this is a decay length and diminishing cooperativity still exists over longer lengths. λ_{eq} in stiff chains, such as double-stranded DNA, is much longer (i.e., n is higher).

It has been observed that the rate of polyelectrolyte interdiffusion in polyelectrolyte complexes[30,31] and PEMUs[25,29,35] is a nonlinear function of salt concentration. An approximate scaling behavior of interdiffusion vs extrinsic ion content may be made with reference to our recent work on transport of multiply charged probe ions within PEMUs.[47] Probe ion hopping is promoted by extrinsic charges forming (random) clusters (a "site") with charge equal to or greater than that of the probe ion.[47] When the ion moves, these extrinsic charges are displaced. The concentration of extrinsic charges, or "doping level", y, is controlled by salt concentration as represented in eq 1. The scaling relationship derived for the probe ion diffusion coefficient was[47]

$$D \sim y^{\nu} \tag{6}$$

where ν is the charge of the probe ion. y is, in turn, controlled by the salt concentration in solution. For the PDADMA/PSS system the approximate relationship is[25]

$$y = 0.2[\mathrm{NaCl}]_{aq} \tag{7}$$

Thus, in the present system, we treat a polyelectrolyte segment of length λ_{eq} as the interdiffusing "unit", and the scaling relationship is

$$D_{\mathrm{PDADMA/PSS}} = 7.1 \times 10^{-17}[\mathrm{NaCl}]_{aq}^{\lambda_{eq}} \tag{8}$$

Equation 8 includes a proportionality constant, as we have one absolute bulk diffusion coefficient from the present work. The scaling power will depend on the λ_{eq}, and the proportionality constant will depend on the ease of PEMU swelling (doping) by salt. PDADMA/PSS is in the "intermediate" swelling range of multilayers,[25] whereas PAH/PSS forms much stronger ion pairs, requiring much higher concentrations of salt, or more aggressive (e.g., hydrophobic or multiply charged) ions

Scheme 3. Adsorption of a Layer during PEMU Assembly[a]

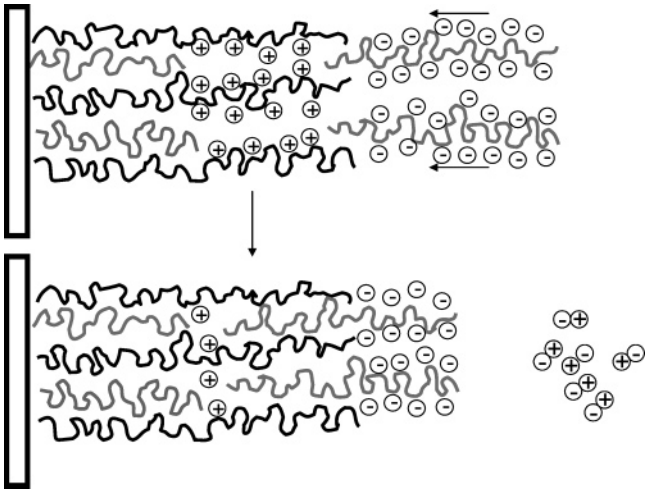

[a] Solid black chains represent negative polymers and faded gray represent positive polymers. The scheme shows intrinsically compensated regions of polyelectrolyte complex (on the left side) and an extrinsically compensated region on the right (the surface). Adsorption of the incoming positive polymer displaces some of the extrinsic charge within the film, creating a new zone of such charge at the new surface. In this idealized scheme, the polyelectrolyte chains, which are in reality oriented more randomly, are shown perpendicular to the substrate so the extrinsic charge layer may be more easily recognized.

to dope to a level where sufficient polyelectrolyte ion pairs are broken to allow mobility.[25] It is perhaps for this reason that structural rearrangements in the much-studied PSS/PAH system have not yet been reported. By contrast, poly(acrylic acid), PAA, a hydrophilic polyelectrolyte, forms easily swelled PEMUs (weaker polyelectrolyte ion pairing is present).[25] PAA multilayers should yield measurable interdiffusion at lower salt concentration. High mobility has been demonstrated for certain other multilayers made with hydrophilic polyelectrolytes.[12−18]

The model considered in relation to Scheme 3 is an "inchworm" model, where a correlated run of repeat units in a loop move along a concentration gradient aided by clusters of counterions, like toothpaste being squeezed from a tube. A literature concept of relevance here is the diffusion of a polyelectrolyte into an oppositely charged gel. Kabanov, Zezin, and co-workers[30,32,56] recognized the importance of extrinsic charge in assisting a charged macromolecule diffuse into an oppositely charged gel, causing collapse in the process. Counterions from the bulk of the gel are thought to be extruded in a "relay race" mechanism as the invading polyelectrolyte displaces them.[32]

Proposed internal structuring, such as that in Figure 2, leads to an interesting paradox when viewed in light of the process of salt-induced annealing (Figure 4): if salt is used in the buildup solutions, why is internal layering not completely eliminated during PEMU construction? It is generally accepted that the surface of a PEMU is rich in extrinsic charge.[5,9,27] According to a recent model,[9] this extrinsic charge is spread out over a few nominal layers, characterized by a penetration length, and is reversed when the system is immersed in a solution of oppositely charged polyelectrolyte. Because of the presence of these extrinsic sites, polyelectrolyte interdiffusion at the surface is enhanced compared to that in the bulk. A simplified representation of the process is depicted in Scheme 3, which shows positive polyelectrolyte (e.g., PDADMAC), together with negative counterions, diffusing into the negative surface of a PEMU during adsorption of one "layer" of positive polyelectrolyte. For most of the adsorption, the surface polymer is in the presence of extrinsic charge; thus, most of the adsorption proceeds rapidly. As the cations are extruded, the level of extrinsic compensation drops, as does the diffusion rate (in a nonlinear fashion). Adsorbing polymer quickly becomes frozen in place. This mechanism ties together observations that a limited buildup of polyelectrolyte is due to a layer of surface excess charge, but long-term adsorption is still seen.[10,57] There is a "rapid" initial phase of adsorption for a layer (rapid because of the presence of surface extrinsic sites) and a much slower second phase of continued adsorption (due to the few extrinsic sites caused by bulk swelling from salt).

Another way of understanding the logic above is by considering that a multilayer built at 0.1 M NaCl takes salt of order 0.8 M to destroy the internal fuzzy layering on the time scale of multilayer construction. Surface diffusion, on the other hand, is much faster than bulk diffusion due to the greater population of extrinsic charge. Given the scaling relationship of eq 8, and $\lambda_{eq} \approx 4$, it may be surmised that y at the surface must be 6 times what it is in the bulk for 0.8 M salt to give diffusion coefficients that are 3 orders higher than those of the bulk.

These arguments also help to understand the unexpectedly narrow character of the Gaussian distribution of d-PSS in Figure 2. The initial stages of adsorption are under conditions where the surface extrinsic charge "forces" interdiffusion (blending) of the adsorbing polymer. When that polymer is fully blended, it diffuses much more slowly. It appears that multilayers may be better layered than previously assumed. During assembly, a small amount of residual extrinsic charge is "marooned" within the multilayer.[11] The enhanced mobility induced by exposure to higher concentration salt solutions, postdeposition, causes better balancing of polyelectrolyte charge and a decrease in this residual extrinsic charge.

Conclusions

The internal layering of polyelectrolytes within multilayers, already diffuse, may be further disordered under the influence of external ionic strength. The decay of coherent neutron reflectivity as a function of annealing time was evaluated using a straightforward self-diffusion limited band spreading model. Polyelectrolyte interdiffusion at the multilayer surface, both perpendicular to the substrate (for adsorbing polymer) and parallel to the substrate (for smoothing of surface topology), is enhanced relative to bulk multilayer diffusion due to the presence of additional extrinsic charge at the surface. Further studies probing diffusion coefficients at different salt concentrations would be helpful for illuminating the nonlinear qualities of salt-induced lubrication of polyelectrolyte interdiffusion. Salt concentration is one variable of many available for controlling whether a multilayer is grown under kinetically locked (linear growth) or labile (exponential growth) conditions. Other factors promoting greater swelling and thus increased mobility are increased temperature,

adding an organic solvent, using hydrophobic counterions, using polyvalent counterions, and ionizing pH-dependent functional groups.

Acknowledgment. This work was supported, in part, by a grant from the National Science Foundation (DMR-0309441). This material is based on work partially supported by the National Institutes of Health under Grant 1 R01 RR14812 and The Regents of the University of California. We thank the CNBT consortium, located at the NIST Center for Neutron Research, for beam time, and in particular U. Perez-Salas for assistance with the neutron experiments, D. J. McGillivray for help with the data modeling, and M. Lösche for critically reading the manuscript.

Supporting Information Available: Details on fitting and profiles. This material is available free of charge via the Internet at http://pubs.acs.org.

References and Notes

(1) Decher, G., Schlenoff, J. B., Eds.; *Multilayer Thin Films—Sequential Assembly of Nanocomposite Materials*; Wiley-VCH: Weinheim, Germany, 2003.
(2) Lvov, Y.; Decher, G.; Haas, H.; Möhwald, H.; Kalachev, A. *Physica B* **1994**, *198*, 89.
(3) Decher, G.; Lvov, Y.; Schmitt, J. *Thin Solid Films* **1994**, *244*, 772.
(4) Schmitt, J.; Grünewald, T.; Decher, G.; Pershan, P. S.; Kjaer, K.; Lösche, M. *Macromolecules* **1993**, *26*, 7058.
(5) Decher, G. *Science* **1997**, *277*, 1232.
(6) Lösche, M.; Schmitt, J.; Decher, G.; Bouwman, W. G.; Kjaer, K. *Macromolecules* **1998**, *31*, 8893.
(7) Bertrand, P.; Jonas, A.; Laschewsky, A.; Legras, R. *Macromol. Rapid Commun.* **2000**, *21*, 319.
(8) Schlenoff, J. B.; Li, M. *Ber. Bunsen-Ges.* **1996**, *100*, 943.
(9) Schlenoff, J. B.; Dubas, S. T. *Macromolecules* **2001**, *34*, 592.
(10) Dubas, S. T.; Schlenoff, J. B. *Macromolecules* **1999**, *32*, 8153.
(11) Schlenoff, J. B.; Ly, H.; Li, M. *J. Am. Chem. Soc.* **1998**, *120*, 7626.
(12) Lavalle, P.; Gergely, C.; Cuisinier, F. J. G.; Decher, G.; Schaaf, P.; Voegel, J.-C.; Picart, C. *Macromolecules* **2002**, *35*, 4458.
(13) Boulmedais, F.; Ball, V.; Schwinte, P.; Frisch, B.; Schaaf, P.; Voegel, J.-C. *Langmuir* **2003**, *19*, 440.
(14) Schöler, B.; Poptoshev, E.; Caruso, F. *Macromolecules* **2003**, *36*, 5258.
(15) DeLongchamp, D. M.; Hammond, P. T. *Chem. Mater.* **2003**, *15*, 1165.
(16) Lavalle, P.; Vivet, V.; Jessel, N.; Decher, G.; Voegel, J.-C.; Mesini, P. J.; Schaaf, P. *Macromolecules* **2004**, *37*, 1159.
(17) Hübsch, E.; Ball, V.; Senger, B.; Decher, G.; Voegel, J.-C.; Schaaf, P. *Langmuir* **2004**, *20*, 1980.
(18) Lavalle, P.; Picart, C.; Mutterer, J.; Gergely, C.; Reiss, H.; Voegel, J.-C.; Senger, B.; Schaaf, P. *J. Phys. Chem. B* **2004**, *108*, 635.
(19) Picart, C.; Mutterer, J.; Richert, L.; Luo, Y.; Prestwich, G. D.; Schaaf, P.; Voegel, J.-C.; Lavalle, P. *Proc. Natl. Acad. Sci. U.S.A.* **2002**, *99*, 12531.
(20) Mendelsohn, J. D.; Barrett, C. J.; Chan, V. V.; Pal, A. J.; Mayes, A. M.; Rubner, M. F. *Langmuir* **2000**, *16*, 5017.
(21) Sukhishvili, S. A.; Granick, S. *J. Am. Chem. Soc.* **2000**, *122*, 9550.
(22) Dubas, S. T.; Schlenoff, J. B. *Macromolecules* **2001**, *34*, 3736.
(23) Dubas, S. T.; Farhat, T. R.; Schlenoff, J. B. *J. Am. Chem. Soc.* **2001**, *123*, 5368.
(24) Sukhishvili, S. A.; Granick, S. *Macromolecules* **2002**, *35*, 301.
(25) Dubas, S. T.; Schlenoff, J. B. *Langmuir* **2001**, *17*, 7725.
(26) Steitz, R.; Leiner, V.; Siebrecht, R.; von Klitzing, R. *Colloids Surf. A* **2000**, *163*, 63.
(27) von Klitzing, R.; Möhwald, H. *Macromolecules* **1996**, *29*, 6901.
(28) Farhat, T. R.; Schlenoff, J. B. *Langmuir* **2001**, *17*, 1184.
(29) Kovacevic, D.; van der Burgh, S.; de Keizer, A.; Cohen Stuart, M. A. *Langmuir* **2002**, *18*, 5607.
(30) Kabanov, V. A.; Zezin, A. B. *Pure. Appl. Chem.* **1984**, *56*, 343.
(31) Karibyants, N.; Dautzenberg, H. *Langmuir* **1998**, *14*, 4427.
(32) See also Chapter 2 in ref 1 for a comprehensive overview.
(33) de Laat, A. W. M.; van den Heuvel, G. L. T.; Böhmer, M. R. *Colloids Surf., A* **1995**, *98*, 61.
(34) Hoogeveen, N. G.; Cohen Stuart, M. A.; Fleer, G. J. *J. Colloid Interface Sci.* **1996**, *182*, 146.
(35) McAloney, R. A.; Dudnik, V.; Goh, M. C. *Langmuir* **2003**, *19*, 3947.
(36) Tronin, A.; Lvov, Y.; Nicolini, C. *Colloid Polym. Sci.* **1994**, *272*, 1317.
(37) Korneev, D.; Lvov, Y.; Decher, G.; Schmitt, J.; Yaradaikin, S. *Physica B* **1995**, *213*, 954.
(38) Kellogg, G. J.; Mayes, A. M.; Stockton, W. B.; Ferreira, M.; Rubner, M. F.; Satija, S. K. *Langmuir* **1996**, *12*, 5109.
(39) Ruths, J.; Essler, F.; Decher, G.; Riegler, H. *Langmuir* **2000**, *16*, 8871.
(40) Arys, X.; Laschewsky, A.; Jonas, A. M. *Macromolecules* **2001**, *34*, 3318.
(41) Buscher, K.; Graf, K.; Ahrens, H.; Helm, C. A. *Langmuir* **2002**, *18*, 3585.
(42) Tarabia, M.; Hong, H.; Davidov, D.; Kirstein, S.; Steitz, R.; Neumann, R.; Avny, Y. *J. Appl. Phys.* **1998**, *83*, 725.
(43) Although the alkanethiol treatment renders the Si wafer surface neutral and hydrophobic, the adsorption of a single layer of PEI worked surprisingly well in "priming" the surface for further PEMU buildup, as evidenced by the quality of the final multilayers.
(44) Tran, Y.; Auroy, P. *J. Am. Chem. Soc.* **2001**, *123*, 3644.
(45) Kiessig, H. *Ann. Phys.* **1931**, *10*, 769.
(46) von Klitzing, R.; Möhwald, H. *Langmuir* **1995**, *11*, 3554.
(47) Farhat, T. R.; Schlenoff, J. B. *J. Am. Chem. Soc.* **2003**, *125*, 4627.
(48) Jaber, J.; Schlenoff, J. B. *Macromolecules* **2005**, *38*, 1300.
(49) The "range" for interpenetration/interdiffusion depends, of course, on how it is defined and how it is measured. For the structural model here, a $\pm 2\sigma$ range would be ± 37 Å, which corresponds to about ± 1.5 "pure" layers of d-PSS. Without knowing the distribution of actual material, it is difficult to relate this interpenetration to that measured by electrochemical means (see for example: Laurent, D.; Schlenoff, J. B. *Langmuir* **1997**, *13*, 1552).
(50) Farhat, T.; Yassin, G.; Dubas, S. T.; Schlenoff, J. B. *Langmuir* **1999**, *15*, 6621.
(51) Walpole, R. E.; Myers, H. R.; Myers, S. L. *Probability and Statistics for Engineers and Scientists*; Prentice Hall: Englewood Cliffs, NJ, 1998.
(52) Szyk; S. P.; Voegel, J.-C.; Schaaf, P.; Tinland, B. *J. Phys. Chem. B* **2002**, *106*, 6049.
(53) Zelikin, A. N.; Trukhanova, E. S.; Putnam, D.; Izumrudov, V. A.; Litmanovich, A. A. *J. Am. Chem. Soc.* **2003**, *125*, 13693.
(54) Kriz, J.; Dybal, J.; Dautzenberg, H. *J. Phys. Chem. A* **2001**, *105*, 593.
(55) Tsuchida, E.; Osada, Y. *Makromol. Chem.* **1974**, *175*, 593.
(56) Chupyatov, A. M.; Rogacheva, V. B.; Zezin, A. B.; Kabanov, V. A. *Polym. Sci.* **1994**, *36*, 169.
(57) Breit, M.; Gao, M.; von Plessen, G.; Lemmer, U.; Feldmann, J.; Cundiff, S. T. *J. Chem. Phys.* **2002**, *117*, 3956.
(58) Schlenoff, J. B. Chapter 4 in ref 1.

MA050072G